

PAPER • OPEN ACCESS

## EBSD analysis of the structure of a weld joining a chromium-nickel steel sheet and a titanium alloy sheet through a copper insert

To cite this article: N B Pugacheva *et al* 2019 *IOP Conf. Ser.: Mater. Sci. Eng.* **681** 012034

View the [article online](#) for updates and enhancements.

**INTERNATIONAL OPEN ACCESS WEEK**  
OCTOBER 19-26, 2020

**ALL ECS ARTICLES. ALL FREE. ALL WEEK.**  
[www.ecsdl.org](http://www.ecsdl.org)

**NOW  
AVAILABLE**

# EBSD analysis of the structure of a weld joining a chromium-nickel steel sheet and a titanium alloy sheet through a copper insert

N B Pugacheva<sup>1</sup>, N S Michurov<sup>1</sup>, and E I Senaeva<sup>1,2</sup>

<sup>1</sup>Institute of Engineering Science, Ural Branch of the Russian Academy of Sciences, 34 Komsomolskaya St., 620049, Ekaterinburg, Russia,

<sup>2</sup>B.N. Yeltsin Ural Federal University, 19 Mira St., Ekaterinburg, 620002, Russia

E-mail: nat@imach.uran.ru

**Abstract.** The structure of the different zones of a CO<sub>2</sub> laser welded joint between a chromium-nickel steel sheet and a titanium alloy sheet, with a copper insert between them, is studied by EBSD analysis. The phase compositions of all the zones have been determined. The weld material has been found to consist of a Cu-based solid solution and unevenly distributed intermetallic particles of different stoichiometric compositions. The heat-affected zones consist of supersaturated iron- and titanium-based solid solutions. After laser welding, the microdeformations of the phase lattices are distributed unevenly over the cross section of the welded joint; namely, the maximum microdeformations and the resulting microstresses are concentrated in the heat-affected zone at the boundary between the weld and the titanium alloy.

## 1. Introduction

The application of the EBSD technique to analyzing the structural state of materials is becoming increasingly popular. This technique is mainly applied to the analysis of deformed alloys and less often to the study of cast alloys and welds. It is promising to use recrystallization and stress maps, as well as the analysis of the textures of the zones of welded joints produced by high-energy radiation sources, e.g. laser and electron-beam ones [1, 2]. When these heat sources are used, high solidification rates, together with convective mixing of the melt in the weld pool, may cause the formation of significant residual stresses and microstrains in welds, particularly if dissimilar materials are to be joined, when heterophase structures are formed.

The aim of this study is to investigate the structural state of the different zones of a laser-welded joint between a chromium-nickel steel and a titanium alloy with an intermediate copper insert.

## 2. Materials and research methods

We studied a weld produced by laser welding of 3 mm thick sheets of the 12Kh18N10T chromium-nickel steel and the VT1-0 titanium alloy with an intermediate copper insert (99.9 wt% Cu). The welding was performed with a continuous CO<sub>2</sub> laser in the Khristianovich Institute of Theoretical and applied Mechanics, SB RAS (Novosibirsk). A mixture of carbon dioxide and air was used to protect the surface of the weld pool and the overheated heat-affected zones. The welding speed was  $V = 1.0$  m/min, the laser radiation power was  $W = 2.3$  kW, and the focal distance was  $F = -2$  mm. The phase composition of the weld and the heat-affected zones was determined with the application of the procedure of electron backscatter diffraction (EBSD) analysis using the Aztec software and a



Tescan Vega II XMU scanning electron microscope equipped with an Oxford NordlysMax<sup>2</sup> device. The electron-probe microanalysis was performed using an INCA Energy 450 device for energy-dispersive microanalysis with an ADD detector.

### 3. Results and discussion

Due to the rapid convective mixing of the melt in the weld pool under the action of a laser beam [1, 2], there occurs mutual penetration of the steel, copper insert, and titanium alloy elements in the entire volume of the pool. As the melt cools, first the intermetallics solidify and then the copper-based solid solution does. According to the data of the electron-probe microanalysis, the copper-based solid solution is significantly supersaturated with iron, chromium, and titanium [2, 3]. High cooling rates, about 1000 °/s, prevent titanium, iron, and copper from binding completely into intermetallics; therefore, the copper-based solid solution contains up to 10 wt% of iron and titanium. The phase EBSD analysis has demonstrated that the intermetallics in the weld material have different stoichiometric compositions, see Fig.1. Near the boundary between the weld and the titanium alloy there is a practically continuous chain of Ti<sub>2</sub>Cu, Ti<sub>3</sub>Cu<sub>4</sub> and TiFe intermetallics. The presence of a 100 to 150 μm thick intermetallic layer in the weld on the side of the titanium alloy was reported earlier in [4].

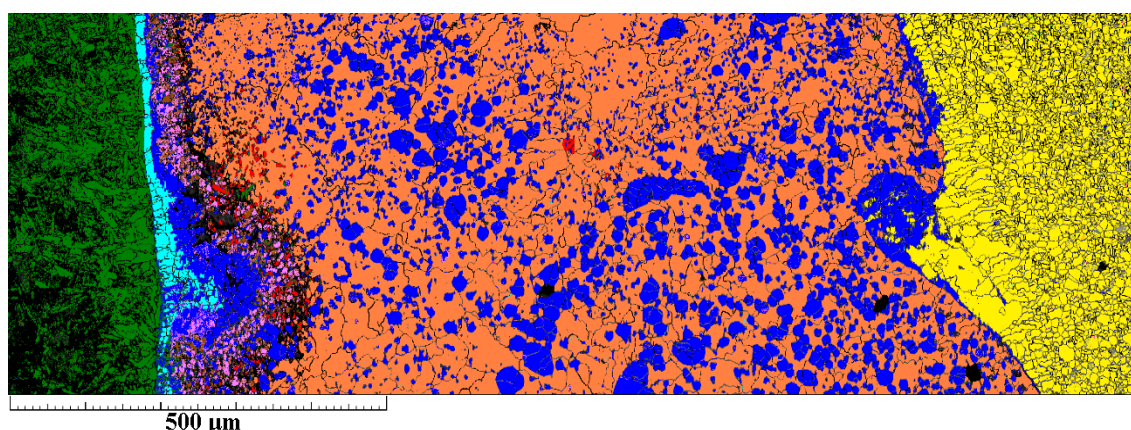


**Figure 1.** The phase composition of the weld: titanium alloy (green), Ti<sub>2</sub>Cu (turquoise), Ti<sub>3</sub>Cu<sub>4</sub> (pink), TiCu (brown), Ti<sub>2</sub>Fe (red), TiFe (blue), steel (yellow), and copper-based solid solution (orange).

The thickness of the intermetallic layer found in the weld ranged between 70 and 180 μm. The intermetallic particles are arranged in layers as follows: right on the boundary with the titanium alloy there is a layer of CuTi<sub>2</sub> intermetallic particles, and then there come the TiFe layer and the layer consisting of a mixture of Ti<sub>3</sub>Cu<sub>4</sub> and TiCu intermetallic particles; the intermetallic layer is followed by the weld material consisting of TiFe, Ti<sub>2</sub>Fe intermetallics uniformly distributed in the Cu-based solid solution, Fig. 1.

The titanium alloy material is constituted by polyhedral grains of the α-phase, Fig. 2a. The analysis of the recrystallization maps has shown that recrystallized grains prevail in it (blue in Fig. 2c) and that there is a small amount of the subgrain and deformed structure (yellow and red, respectively). In the heat-affected zone the structure of the titanium alloy consists of packet and polyhedral grains of the α-phase, Fig. 2b. Due to high heating and cooling rates, as well as owing to the polymorphic β→α transformation under cooling after welding, there are fewer recrystallized grains in this zone, grains with a subgrain structure (yellow in Fig. 2d) and deformed ones (red in Fig.2d) prevail.

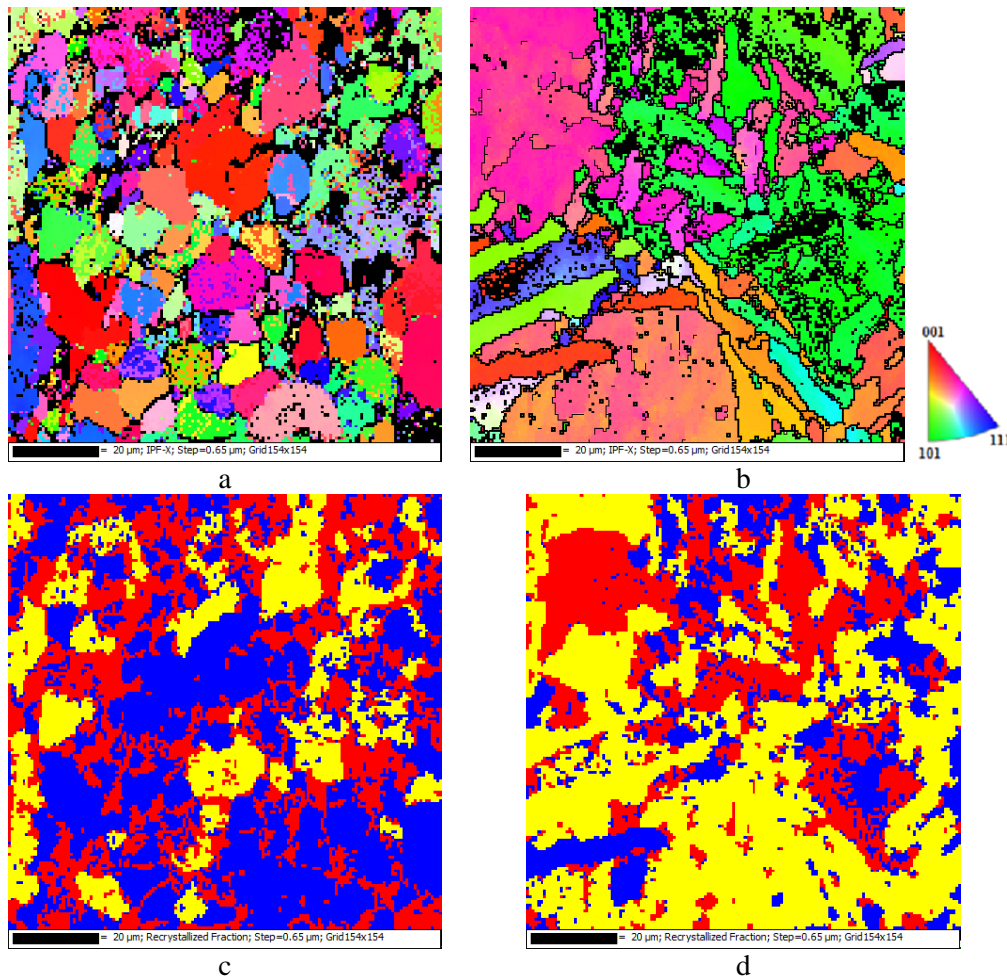


**Figure 2.** The microstructure (a, b) and recrystallization maps (c, d) of the titanium alloy in the initial state (a, c) and in the heat-affected zone (b, d); deformed grains (red in c and d), recrystallized grains (blue), and subgrains (yellow).

The electron-probe microanalysis of the titanium alloy near the weld has shown the presence of such alloying elements as Fe, Cu, Cr, and Ni in the titanium solid solution (Fig.3 a, the green, violet, red, and yellow lines, respectively), which act as stabilizers of the  $\beta$ -phase in titanium (). To determine the possibility of  $\beta$ -Ti stabilization in the heat-affected zones, we used a molybdenum equivalent  $Mo_{eq}$  [4, 5]:

$$Mo_{eq} = \sum \frac{x_i \cdot C_{Mo}''}{C_i''} = \%Mo + \frac{\%Ta}{4.5} + \frac{\%Nb}{3.6} + \frac{\%W}{2.25} + \frac{\%V}{1.5} + \frac{\%Cr}{0.63} + \frac{\%Mn}{0.65} + \frac{\%Fe}{0.35} + \frac{\%Co}{0.7} + \frac{\%Ni}{0.9}$$

As a result, the value of the molybdenum equivalent  $Mo_{eq}$  of the heat-affected zone proves to be equal to 20.9%; this corresponds to pseudo- $\beta$ -titanium alloys, for which a  $\beta$ -structure is fixed during hardening. The EBSD study of the region under study has verified the presence of a solid solution of the alloying elements in the  $\beta$ -titanium at the boundary between the titanium alloy and the weld, with uniformly arranged TiFe and  $Ti_2Cu$  intermetallics and inclusions of the Cu-based solid solution (Fig. 3b).

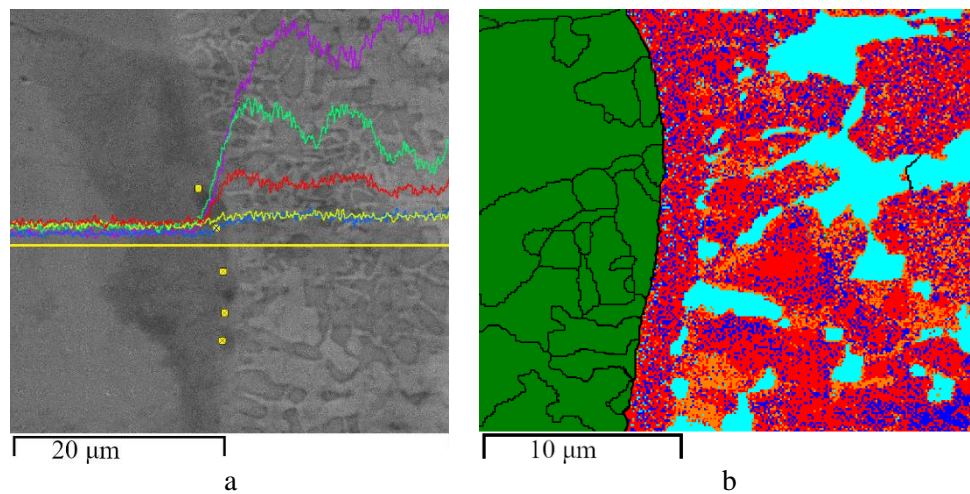


**Figure 3.** The boundary between the titanium alloy and the weld: the distribution of the chemical elements along the line and the areas of local analysis (a); the phase composition of the boundary between the weld and the titanium alloy (green –  $\alpha$ -Ti, red –  $\beta$ -Ti, orange – Cu, blue – TiFe, turquoise –  $\text{Ti}_2\text{Cu}$ ) (b).

**Table 1** – Averaged values of the content of the chemical elements in the titanium alloy at the boundary with the weld

Element	Si	Ti	Cr	Mn	Fe	Ni	Cu
wt%	0.1	74.4	1.9	0.1	5.9	0.8	16.8

In the central part of the weld the TiFe, TiCu, and  $\text{Ti}_3\text{Cu}_4$  intermetallic particles (Fig. 4a) do not form clusters, they are distributed at some distance from each other in the Cu-based solid solution. The Cu-based solid solution grains are deformed after laser welding (red in Fig. 4b), whereas the intermetallics remain undeformed due to their high hardness and strength, and in the analysis of the recrystallization maps obtained by the EBSD technique they are qualified as recrystallized (blue in Fig. 4b). It was reported in [6] that the intermetallic particles chaotically arranged and distributed in the solid solution contribute to a decrease in the total level of strains and residual stresses due to their redistribution and dissipation in the weld volume. Thus, in the weld material there are no stress concentrators able to accelerate failure caused by external loads.

In the heat-affected zone on the side of the steel there prevails a subgrain structure. At the boundary between the weld and the steel the TiFe and TiCu intermetallic particles do not form continuous chains (Fig. 1). The analysis of the stress map has shown that no critical maximum stresses arise after welding, Fig. 5. Although the weld zone contains a considerable number of intermetallic particles, maximum microstrains after laser welding appear in the heat-affected zone on the side of the titanium alloy, Fig. 5.



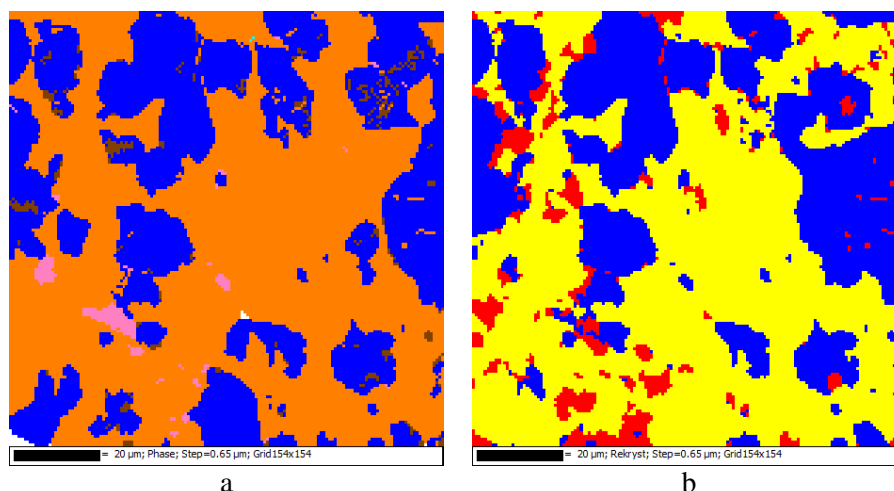


**Figure 4.** The phase composition (a) and recrystallization maps (b) of the weld material: (a) – the Cu-based solid solution (orange), TiFe (blue),  $\text{Ti}_3\text{Cu}_4$  (pink), and TiCu (brown); (b) – deformed grains (red), recrystallized grains (blue), and subgrains (yellow)

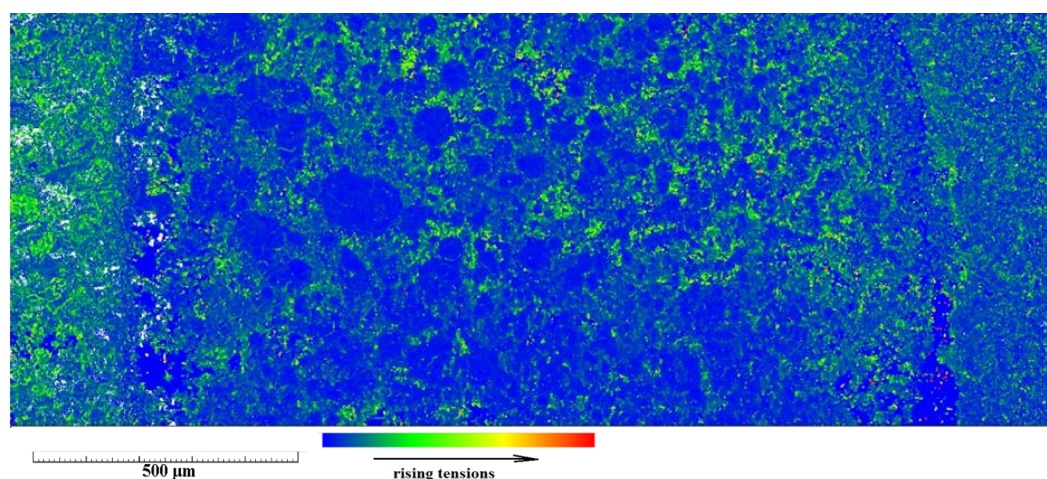


**Figure 5.** Stress maps for the weld joining chromium-nickel steel and titanium alloy sheets through a copper insert

#### 4. Conclusion

The EBSD analysis has demonstrated that the weld joining the 12Kh18N10T and the VT1-0 alloy through a copper insert consists of a Cu-based supersaturated solid solution and  $\text{Ti}_2\text{Cu}$ ,  $\text{Ti}_3\text{Cu}_4$ , TiCu,  $\text{Ti}_2\text{Fe}$ , and TiFe intermetallic particles. Near the boundary with the titanium alloy the intermetallic particles are arranged in layers, whereas in the weld and near the boundary with the steel they are distributed in the solid solution. The doping of the titanium alloy with Cu, Fe, Cr, and Ni transforms it from the  $\alpha$ -alloy into a pseudo- $\beta$ -alloy in the heat-affected zone near the weld. After the welding is completed, high cooling rates and the difference in the thermal coefficients of linear expansion of the phases in the welded joint cause the formation of deformed regions and residual stresses, whose maximum values are concentrated at the boundary between the weld and the titanium alloy.

#### 5. Acknowledgments

The work was performed on the equipment installed in the Plastometriya collective use center of the IES UB RAS within state assignment, theme No. AAAA-A18-118020790145-0.

**References**

- [1] W.W. Duley. Laser Processing an analysis of materials. Pienum Press, New York. 1983. 474.
- [2] Cherepanov A.N., Orishich A.M., Shapeev V.P., and Pugacheva N.B. Thermophysics and aeromechanics 22 (2015) No. 2, 135–142.
- [3] Veretennikova, I., Pugacheva, N., Smirnova, E., and Michurov, N. (2018). The laser-welded joint of an austenitic corrosion-resistant steel and a titanium alloy with an intermediate copper insert. Letters on Materials, 8(1), 42–47.
- [4] Malcher, L. and Mamiya, E. N. (2014). An improved damage evolution law based on continuum damage mechanics and its dependence on both stress triaxiality and the third invariant. International Journal of Plasticity, 56, 232–261.
- [5] Jia, Y. and Bai, Y. (2016). Ductile fracture prediction for metal sheets using all-strain-based anisotropic eMMC model. International Journal of Mechanical Sciences, 115–116, 516–531.
- [6] N. S. Michurov, N. B. Pugacheva, I. A. Veretennikova, Yu. V. Khalevitsky, E. O. Smirnova, and A. S. Igumnov. Contribution of intermetallics to the formation of the stress-strain state of tensile welds on the AISI 321 steel and the grade 2 titanium alloy with a copper insert// AIP Conf. Proc. **2053**, 040058 (2018); doi: 10.1063/1.5084496.